JAST, Vol. 8, No. 2, pp 127–133

JAST Journal of Aerospace Science and Technology

Research Note

Flow Field Characteristics of an Aerospike Nozzle, Using Different Turbulence Models

S. Noori[1] and A. Shahrokhi[2]

To improve the calculation of the flow properties of an aerospike nozzle, different turbulence models were investigated in this study. The primary shape of the nozzle plug is determined through utilizing an approximate method. The flow field is, then, simulated using the Navier-Stokes equations for compressible flows. The commercial computational fluid dynamics code Fluent is used to simulate the flow around an aerospike nozzle. The computational methodology employs steady state density-based formulation and a finite volume cell centered scheme to discretize the flow field equations. To accelerate the solution convergence, the flow field is divided into several zones in order to facilitate each zone with proper unstructured grid and also to offer the appropriate initial conditions for each zone. The accuracy and the robustness of wall function based turbulence schemes, i.e. k-ϵ model, are compared with those of Spalart-Allmaras (S-A) and k-ω turbulence models.

NOMENCLATURE

C_P	specific heat at constant pressure (J/kgK)
F	thrust (N)
h	altitude (m)
I_{sp}	specific impulse (s)
L	length (m)
$\dot{m}$	mass flow rate (kg/s)
M	Mach number
P	absolute static pressure (N/m^2)
T	absolute static temperature (K)
r	radial coordinate
γ	ratio of specific heats
x	axial coordinate

Subscripts

e	exhaust
i	inlet
t	throat
1	stagnation

1. *Assistant Professor, Aerospace Research Institute, Tehran, Iran.*
2. *Ph.D., School of Computing, University of Leeds, UK.*

INTRODUCTION

Conventional bell nozzles suffer from reduced engine performance, *i.e.* overexpansion and under expansion at high and low altitudes correspondingly. To achieve relatively better performance, the aerospike engine has been variously studied since early 60^{th}. This kind of nozzle possesses the best capabilities for continuous altitude compensation due to unbounded expansion of the jet which leads to overall better performance in aerospike nozzles [1].

Since aerospike engines possesse aerodynamic efficiency across a wide range of altitudes, it is a good candidate for space shuttle propulsion systems. However, the technical difficulties of developing spiked nozzles, blocked research on them for a long period of time. The researches on such nozzles became active again in the United States, Europe and, then, in Japan after the resurrection of the aerospike nozzles for reusable launch vehicle propulsion systems [2]. Experimental research on aerospike nozzles and the parametric studies were performed by the Japanese in the mid-90's [3,4]. Further research was carried out using linear aerospike nozzles and the basic characteristics of the aerospike nozzle were obtained [5,6]. In Europe, the Future European Space Transportation Investigations

Program for European Space Agency activated the research on such nozzles in 1998 [7, 8].

Pursuing the research programs, various investigations were conducted by scientists on aerospike nozzles. Frendi and his colleagues investigated the aerospike engine noise both experimentally and computationally [9]. Verma studied the influence of annular conical spike nozzle and compared the performance of this nozzle with conical plug [10]. Wang conducted computational heat transfer analyses to study the effect of the fence on the base heating of an X-33 aerospike engine [11]. Zebbiche investigated the supersonic two-dimensional plug nozzle at high temperatures. The goal of his research was to trace the profiles of the supersonic plug nozzle when this stagnation temperature considered to be lower than the threshold of dissociation of the molecules [12]. For Further numerical analysis, some experimental studies have been done on aerospike nozzles in different structures and working conditions as well[13,14].

As documented in the aerospace literature, the flow in supersonic nozzles is substantially influenced by viscous effects which may reduce the performance of the propulsion system [15]. In many cases, the Reynolds number of the flow over the plug is high enough to oblige a turbulence flow along the nozzle spike. Dai and his group presented numerical and experimental results on a tile-shaped aerospike nozzle. In their computational simulations, they used Reynolds Averaged Navier-Stokes $k-\epsilon$ turbulence model [15]. Koutsavdis applied several turbulence models for computation of a plug nozzle flow field and compared the results with experimental observations [16]. According to Koutsavdis studies about the influence of the flow separation around the boot tail of the truncated nozzle, the $k-\omega$ turbulence model appears to be the model of choice for prediction of most of the characteristics of the flow on the full nozzle. Geron *et.al.* numerically solved the Reynolds averaged Navier-Stockes equations for a linear aerospike whose shape is designed by a two dimensional approach. In their research, Geron and his group considered a compressible inert gas with the Spalart-Allmaras turbulence model [17].

Recently, Zilic numerically examined the thrust performance of the linear aerospike nozzle micro-thruster for various nozzle spike lengths and flow parameters in order to identify optimal geometry and operating conditions [18]. A numerical investigation of external air slipstream effects on the flow properties and thrust performances of the plug nozzle was carried out by Bozic [19]. The analyzed flow constellation with separated flow region around the plug nozzle occurs during the suborbital flight of the small launch vehicle at supersonic and hypersonic velocity in turbulent flow field regime. RANS one-equation Spalart-Allmaras turbulent model was utilized in this research [20].

Besnard and his group studied on the design, manufacturing and test of an annular aerospike engine [21]. They computed the thrust component distribution considering Spalart-Allmaras turbulence scheme.

The focus of the present study is on the flow field computation of an aerospike nozzle using different turbulent models in order to provide some insight into the efficiency of each method on the accuracy of the nozzle thrust and pressure distribution estimations.

GEOMETRY OF THE PLUG NOZZLE

The contours of aerospike nozzles have been traditionally designed by simple methods like method of characteristics and approximate method or more elaborate methods like techniques based on calculus of variations. These approaches determine the aerodynamic contour that approximates a design for maximum thrust at one design condition. Figure 1 shows the aerospike nozzle components which include rocket thruster, cowl, aerospike nozzle and plug base contour.

In this section, an approximate method [22] has been used to design the plug shape at a specified design condition. The approximate method utilizes ideal rocket assumptions to derive a set of analytical relations, which can be used to calculate radius and flow properties at each longitudinal station of the plug [23,24]. The expansion ratio for the given values of combustion chamber pressure and optimum working altitude are calculated using the following relation:

$$\frac{A_t}{A_e}=\left(\frac{\gamma+1}{2}\right)^{\frac{1}{\gamma-1}}\left(\frac{P_e}{P_1}\right)^{\frac{1}{\gamma}}\left[\left(\frac{\gamma+1}{\gamma-1}\right)\left(1-\left(\frac{P_e}{P_1}\right)^{\frac{\gamma-1}{\gamma}}\right)\right]^{1/2} \tag{1}$$

The nozzle throat and exhaust areas for a given value of optimum thrust are determined through Eq. 2:

$$C_F=\left[\frac{2\gamma^2}{\gamma-1}\left(\frac{2}{\gamma+1}\right)^{\frac{\gamma+1}{\gamma-1}}\left(1-\left(\frac{P_2}{P_1}\right)^{\frac{\gamma-1}{\gamma}}\right)\right]^{\frac{1}{2}}=\frac{F}{A_tP_1} \tag{2}$$

where,

$$A_e=\epsilon A_t \tag{3}$$

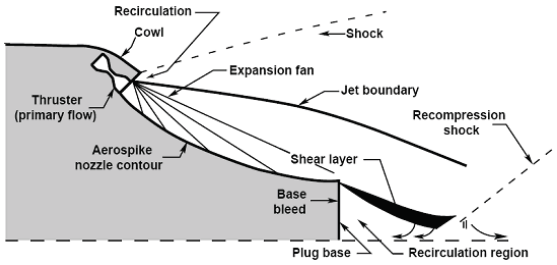

Figure 1. Schematic of the aerospike nozzle components.

The exhaust Mach number for a given expansion ratio is calculated using Eq. 4:

$$\frac{A_e}{A_t} = \frac{1}{M_e}\left[\frac{1+\frac{\gamma-1}{2}M_e^2}{1+\frac{\gamma-1}{2}}\right]^{\frac{\gamma+1}{2(\gamma-1)}} \tag{4}$$

For the exhaust flow to be parallel to the nozzle's axis, the throat must have an angle equal to the Prandtl-Meyer expansion angle corresponding to the exhaust Mach number [21]:

$$\theta_t = v(M_e) = \sqrt{\frac{\gamma+1}{\gamma-1}}\tan^{-1}\sqrt{\frac{\gamma-1}{\gamma+1}(M_e^2-1)} - \tan^{-1}\sqrt{M_e^2-1} \tag{5}$$

The radius of the plug at throat is determined through the following equation:

$$A_t = \frac{\pi\left(r_e^2 - r_t^2\right)}{\cos\theta_t} \tag{6}$$

The local flow angle and area for each station along the plug corresponding to a Mach number between 1 and M_e, are obtained:

$$\mu = \sin^{-1}\tfrac{1}{M},\ v = v(M),\ \theta = \theta_t - v$$
$$\tfrac{A}{A_t} = \tfrac{1}{M}\left[\tfrac{2}{\gamma+1}\left(1+\tfrac{\gamma-1}{2}M^2\right)\right]^{\frac{\gamma+1}{2(\gamma-1)}} \tag{7}$$

The local radius (r) of plug and longitudinal coordinate (x) at the same station are

$$r^2 = r_e^2\left(1 - \frac{A}{A_t}\frac{\sin(\mu+\theta)}{\sin\mu\cos\theta_t}\right) \tag{8}$$

$$x = \frac{r_e - r}{\tan(\mu+\theta)} \tag{9}$$

The calculation of local flow angle, local area for each station along the plug, the local radius (r) of plug and longitudinal coordinate should be repeated incrementally from $M = 1$ up to M_e in order to obtain coordinates of the entire plug.

As mentioned in the introduction, Besnard and his group conducted a thorough computational investigation on annular aerospike nozzle, [21]. In order to ensure the accuracy of the results, the method presented in this section is implemented to design an aerospike nozzle in the 4-5 KN thrust class with specifications originally introduced in [21]. The chamber pressure is 2067857 N/m^2 and the optimum design altitude is 3657.6 m in which the optimum thrust of 4443.9 N is achieved. The specific impulse and mass flow rates are 235 s and 3.258 kg/s respectively. The propellant is ethanol-oxygen with the specific heat ratio of 1.21 and $C_P = 1286.68$ J/kgK.

The nozzle specifications are calculated using the relations presented in this section. The geometrical parameters and the exit Mach number obtained through the approximate method mentioned above are listed below.

Table 1. Aerospike nozzle specifications.

Item	Parameter	Value
1	throat angle	57.17
2	throat radius	0.0452(m)
3	exhaust Mach number	2.804
4	exhaust radius	0.0479(m)

FLUID PROPERTIES AND NUMERICAL METHOD

In order to ease the modeling of the flow properties, average properties of the combustion products of the chemical reaction of ethanol and oxygen have been assumed for the fluids in all regions. These properties are as follows:

$$\gamma = 1.21,\ C_P = 1286.68\ J/kgK,\ M = 37.23\ g/mol.$$

Combustion products have been assumed to follow the ideal gas equation ($P = \rho RT$).

The numerical analysis of the internal and external flow of the aerospike nozzle is performed using Navier-Stokes equations and considering turbulent flow. The governing equations with upside descriptions are:

Continuity

$$\frac{\partial}{\partial t}(\rho) + \nabla.(\rho\vec{v}) = 0$$

Momentum

$$\frac{\partial}{\partial t}(\rho\vec{v}) + \nabla.(\rho\vec{v}\vec{v}) = \nabla p + \nabla.\bar{\bar{\tau}} + \rho\vec{g} + \rho\vec{F}$$

Energy

$$\frac{\partial}{\partial t}(\rho h) + \nabla.(\rho\vec{u}h) = \frac{\partial P}{\partial t} + \bar{\bar{\tau}} : \nabla\vec{u} - \nabla.q + S$$

where, $\vec{v}$, $\bar{\bar{\tau}}$ and F are the velocity vector, stress-strain tensor and external body force respectively.

The governing equations have been solved using the commercial finite-volume based cfd code Fluent [25]. The computational methodology utilizes a steady state density-based formulation and a finite- volume, cell-centered scheme to discretize the flow field equations. Severe compressibility effects exist in the solution domain which rigorously reduce the convergence towards the results. To treat the slow convergence rate, the flow field is divided into several zones. Each zone is assigned with a proper unstructured triangle grid and appropriate initial conditions.

The coupled implicit method has been implemented in order to solve the above governing equations, *i.e.* continuity, conservation of momentum in longitudinal and radial directions, and conservation of energy. The considered Fluxes of convected variables at cell walls are approximated by the first order upwind scheme. Two criteria have been carefully observed for

convergence. One is reduction of the global residual of solution of all governing equations to the order of 10^{-5}, and the other is mass balance among inlet, far-field and outlet boundaries. The latter is checked by integration of mass flow through the mentioned boundaries in each iteration. Although the first criterion is satisfied earlier in most cases, the solution process has been continued until both criteria are satisfied.

The unstructured grid is also used for the solution of Navier-Stokes equations considering turbulent flow in other references [26]. Providing control over the grid density and initial conditions in different zones is helpful in accelerating the solution convergence.

The most complete way of predicting turbulence is to solve for the full Navier-Stokes equations directly using Direct Numerical Simulation (DNS). This technique requires the grid and time steps to be adequately small to obtain accurate results. Consequently, this method is computationally expensive. An alternative approach is Large Eddy Simulation (LES). In LES, large vortexes (eddies) are computed directly, while small scale eddies are modeled. Thus, the space grid and time steps are much larger than those in DNS and fewer computations are performed. Large Eddy simulation has been most successful for high-end applications where RANS models fail to meet the needs, *e.g.* combustion and mixing. Another technique which is practically examined in many engineering applications is Reynolds Average Navier-Stokes (RANS). This technique allows the calculation of mean flow properties in the flow field. The turbulence models are, then, utilized to resolve the near wall turbulence effects. Among turbulence models, Spalart-Allmaras, $k-\epsilon$ and $k-\omega$ are widely used in aerospace applications. The effect of these turbulence models are examined in this research.

Spalart-Allmaras (S-A) one-equation model is one of the methods used for turbulence modeling. The Spalart-Allmaras is a low cost RANS model solving a transport for modified eddy viscosity. This model has been successfully employed by many researchers for turbulence modeling of aerospike base flow [17, 19, 21].

In comparison with one equation turbulence models, two-equation turbulence models are complete, *i.e.* they can be used to predict the properties of a given turbulence flow with no prior knowledge of turbulence structure. Based on the physical specifications of the flow, the flow field computations are repeated using $k-\epsilon$ and $k-\omega$ turbulence schemes. The $k-\epsilon$ model is the most widely used engineering turbulence model for industrial applications. This model is robust and reasonably accurate. This method is shown to obtain reasonable results in the modeling of aerospike nozzle flows in the case of a truncated nuzzle base [22,15].

The $k-\omega$ turbulence model equations do not contain terms which are undefined at the wall without using wall functions. This model is accurate and robust for a wide range of flows with a pressure gradient. Also $k-\omega$ turbulence model is most widely adopted in the aerospace communities. More information about different turbulence models can be found in [27].

RESULTS AND DISCUSIONS

This section describes numerical modeling and analysis of the internal and external flow of the aerospike nozzle introduced previously. The results presented in this section are obtained using a commercial CFD code. The results are obtained in the design conditions of the nozzle where the exit pressure equals the ambient pressure. The objective of the analysis is to evaluate the effect of the turbulence models in the calculated aerospike nozzle thrust.

Turbulent intensity and length scale are 1% and 0.001m for three turbulent models in this paper. In order to investigate the role of the turbulence cases in

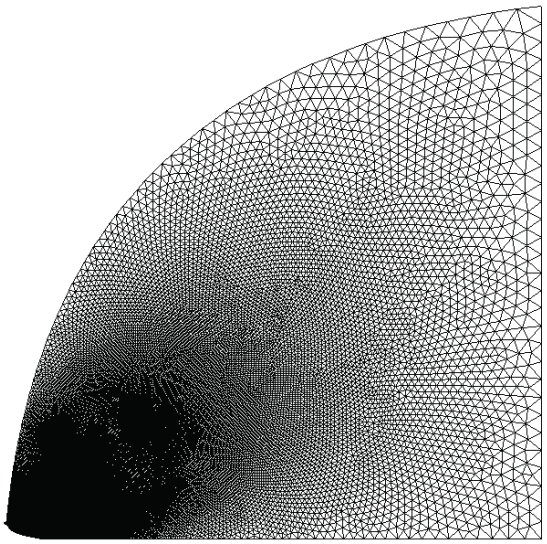

Figure 2. Grid Distributions in the flow field.

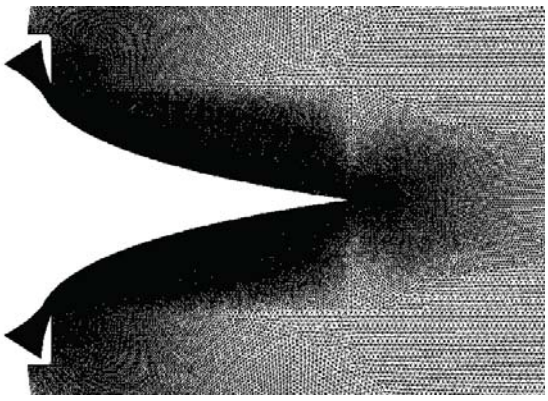

Figure 3. Grid Distributions in the convergent part of the nozzle and along the plug.

the accuracy of the results, a laminar case is studied as well. The numerical results are validated against the computed thrust in Ref. 19 for the design conditions $P_{atm}/P_{design} = 1.0$ where the optimum thrust is 4443.93 N. The inlet properties of the convergent part considered here are

$L = 0.2\,m$

$A_i = 7.21285510^{-3} m^2$

$A_i/A_t = 5.01384$

$M_i = 0.13$

$P_i = 0.98984$

The grid independency is checked using different resolutions yielding 1051312, 149644, 188517, 191097, and 257895 cells and the computed thrust force for each case is 2965.94 N, 3151.68 N, 3282.03N, 3283.86 N and 3285.21 N respectively (Table 2). Therefore, the third case is chosen as the most appropriate resolution. The entire solution domain is displayed in Figure 2. The solution domain has been divided into 4 regions to provide the solution domain with different initial conditions defined in each region. The numerical solution is carried out in half of the entire domain due to axial symmetry of the problem. Figure 3 shows the grid distribution in the convergent part of the nozzle and near the plug. The grid density increases towards the throat and the remaining computational domain coarseness increases outward from the nozzle outlet. To meet the requirement for Y^+ parameter in different kinds of turbulence modeling, the grid coarseness is modified near the wall for each turbulence model.

Figure 3 shows the resulting grid in the vicinity of the aerospike nozzle. The average properties of combustion products resulting from the chemical reaction of ethanol and oxygen is assumed for the entire fluids in all regions. The boundary condition at the inlet of the convergent section is the specified mass flow of 3.25757 kg/s with the total temperature of 1577.826 K.

The main characteristic of the exhaust flow of the aerospike nozzle is the formation of a series of expansion waves emanating from the upper lip of the convergent part of the nozzle. Contrary to the conventional nozzles, the exhaust flow is not limited to a solid wall. So in the case of a plug nozzle, the expansion waves can adjust their intensity and domain to match with the external flow. In the present case in which the exit pressure equals the ambient pressure, the expansion waves are expected to persist up to the end of the spike.

Table 2. Grid study.

No. of cells	1051312	149644	188517	191097	257895
Thrust force (N)	2965.94	3151.68	3282.03	3283.86	3285.21

The convergent nozzle first cell Y^+ values for k-å turbulence model are shown in Figure 4. In this figure, the value of x axis is negative because of the location of the coordinate origin. The Y^+ values are limited to about 130 which is acceptable due to using wall function in the viscous sub-layer near the wall. The total thrust force is 4414.79N.

First cell Y^+ values distribution is provided in Figure 5 in the case of $k-\epsilon$ turbulence model. The total thrust force obtained using $k-\omega$ scheme is 4437.53N.

Y^+ values for the convergent nozzle wall are show in Figure 6. The total thrust force is 4429.08 N. To realize the influence of the turbulence modeling in the flow field properties, the flow is resolved considering laminar boundary layer. The thrust force in the laminar case is 4393.21 N. The computation is made on an Intel Core i7 processor with RAM of 2GB. The CPU time required for the present case is 43200s.

Three thrust components and the total thrust forces are tabulated in Table 3. The results are improved when the turbulence model is considered in the numerical calculations. The best and worst results are obtained when $k-\omega$ scheme and laminar cases are respectively used.

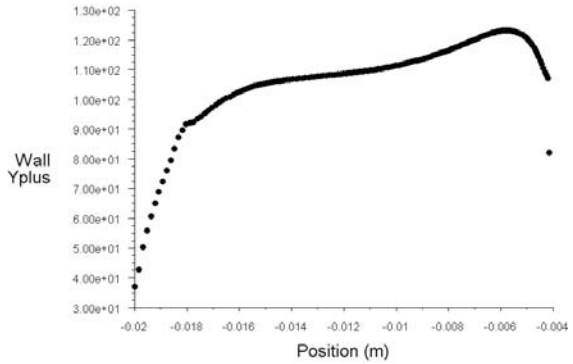

Figure 4. Convergent nozzle wall Y^+ Curve, RNG $k-\epsilon$.

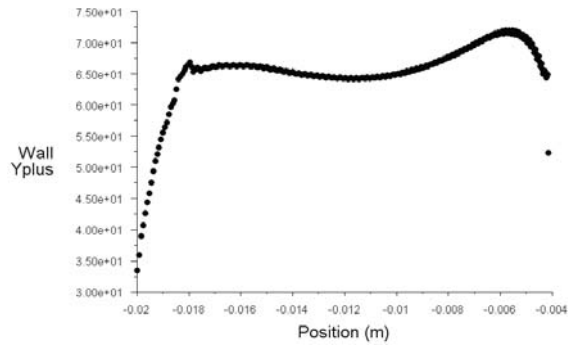

Figure 5. Convergent nozzle wall Y^+ Curve, $k-\omega$.

Table 3. Thrust of the aerospike nozzle in different Flow Solver Model.

Flow Solver Model	T1	T2	T3	Total Thrust	Difference with Thrust from ref [18](%)
$K-\epsilon$ (RNG)	987.24	953.69	2473.86	4414.79	0.65
$K-\omega$	993.32	956.07	2488.14	4437.53	0.14
S-A	977.66	961.00	2490.42	4429.08	0.33
Laminar	968.0	962.14	2463.07	4393.21	0.93

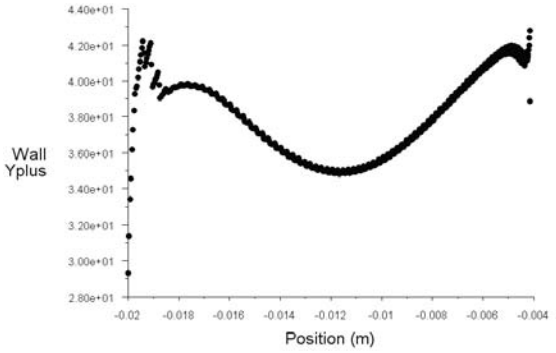

Figure 6. Convergent nozzle wall Y^+ Curve, Spalart-Allmaras.

CONCLUSION

Different turbulence models were used to examine the influence of the turbulence modeling in the flow field properties and also to compare the result of each method with that of others. The flow properties appeared to be similar in the overall view of the contours. In all cases, the expansion waves continued until the end of the plug as expected for the considered pressure ratio. In the case of laminar flow, the Mach and pressure contours were notably different with $K-\omega$ and S-A turbulent cases. Also, the total thrust forces are determined using different turbulence models. It is concluded that the thrust force is more accurate when turbulence model is employed in the numerical calculations.

REFERENCES

1. Pires M., "Turbulence Modeling and Applications to Aerospike Plug Nozzle", *26^{th} International Congress of the Aeronautical Sciences*, (2008).
2. Ito T. and Fujii K., "Flow Field and Performance Analysis of Aerospike Nozzles with Simplified Clustered modules", *Transactions of the Japan Society for Aeronautical and Space Sciences, TRANS JPN SOC AERON SPACE*, **47**(155), PP 17-22(2004).
3. Ito T., Fujii K. and Hayashi A.K., "Computations of the Axisymmetric Plug Nozzle Flow Fields", *Journal of Propulsion and Power*, **18**(2), PP 354-260(2002).
4. Tomita T., Tamura H. and Takahashi M., "An Experimental Evaluation of Plug Nozzle Flow Fields", *Proceeding of AIAA, ASME, SAE, and ASEE, Joint Propulsion Conference and Exhibit*, (1996).
5. Onodera T., Tomita T. and Tamura H., "Numerical Investigation of the Flow Field around Linear Aerospike Nozzles", *35th AIAA/ASME/SAE/ASEE Joint Propulsion Conference and Exhibit*, Los Angeles, California, (1999).
6. Sakamoto H., Takahashi M., Sasaki M., Tomita T., Kusaka K. and Tamura H., "An Experimental Study on a 14kN Linear Aerospike Nozzle Combustor", *Proceedings of the Conference on Aerospace Propulsion*, **39**, (1999).
7. Vuillamy D. and Duthoit V., "European Investigation of Clustered Plug Nozzles", *Proceedings of the 35th AIAA/ASME/SAE/ASEE Joint Propulsion Conference and Exhibit*, Los Angeles, California, (1999).
8. Hagemann G., Immich H. and Terhardt M., "Flow Phenomena in Advanced Rocket Nozzles – The Plug Nozzle", *Proceedings of the 34th AIAA/ASME/SAE/ASEE Joint Propulsion Conference & Exhibit*, Cleveland, OH, (1998).
9. Frendi A., Nesman T. and Wang T., "Computational and Experimental Study of Linear Aerospike Engine Noise", *AIAA Journal*, **39**(8), PP 1485-1492(2001).
10. Verma S.B., "Performance Characteristics of Annular Conical Aerospike Nozzle with Free Stream Effect", *Journal of Propulsion and Power*, **26**(3), (2009).
11. Wang T., "Effect of Fence on Linear Aerospike Plume-Induced Base-Heating Physics", *Journal of Thermo physics and Heat Transfer*, **14**(4), PP 457-463(2000).
12. Zebbiche T. and Youbi Z., "Supersonic Two-Dimensional Plug Nozzle Conception at High Temperature", *Emirates Journal for Engineering Research*, **11**, PP 77-89(2006).
13. Ruf J.H. and McDaniels D.M., "Experimental Results for an Annular Aerospike with Differential Throttling", *5^{th} International Symposium on Liquid Space Propulsion*, Chattanooga, TN, (2003).
14. Ruf J.H., Hagemann G. and Immich H., "Comparison of Experimental Data and Computations Fluid Dynamics Analysis of a Three Dimensional Linear Plug Nozzle", *39^{th} AIAA/ASME/SAE/ASEE Joint Propulsion Conference and Exhibit*, Huntsville, Al;United States, (2003).
15. Dai W., Liu Y. and Cheng X., "Analytical and Experimental Studies of Tile-Shaped Aerospike Nozzles", *Journal of Propulsion and Power*, **19**(4), PP 640-645(2003).
16. Koutsavdis E.K., "A Numerical Investigation of the Flow Characteristics of Plug Nozzle Using Fluent", *Proceedings of the 40^{th} AIAA meeting and exhibition*, Reno, NV, (2002).

17. Geron M., Paciorri R., Nasuti F., Sabetta F. and Martelli E., "Transition between Open and Closed Wake in 3d Linear Aerospike Nozzles", *41st AIAA/ASME/SAE/ASEE Joint Propulsion Conference & Exhibit*, Tucson, Arizona, (2005).

18. Zilic A., Hitt D.L. and Alexeenko A.A., "Numerical Simulations of Supersonic Flow in a Liear Aerospike Micronozzle", *37th AIAA Fluid Dynamics Conference and Exhibit*, Miami, FL, (2007).

19. Bozic O. and Porrmann D., "Estimation of Flow Field Properties and Thrust Performances of Axisymmetric Plug-Nozzles using CFD Simulations", *Turbulence, Heat and Mass Transfer*, **6**, (2009).

20. Deck S., Espiney P.D. and Guillen P., "Development and Application of Spalart-Allmaras one Equation Turbulence Model to Three-Dimensional Supersonic Complex Configuration", *Aerospace Science and Technology*, PP 171-183(2002).

21. Besnard E., Chen H.H., Mueller T. and Garvey J., "Design, Manufacturing and Test of a Plug Nozzle Rocket Engine", *Proceedings of the 38th AIAA/ASME/SAE/ASEE Joint Propulsion Conference & Exhibit*, (2002).

22. Angelino G., "Approximation Method for Plug Nozzle Design", *AIAA Journal*, **2**(10), PP 1834-1835(1964).

23. Greer H., "Rapid Method for Plug Nozzle Design", *ARS Journal*, PP 560-561(1971).

24. Sutton G.P. and Biblarz O., *Rocket Propulsion Elements*, 7th Edition, John Wiley & Sons, Inc., (2000).

25. Fluent Software, "version 6.3.26", .

26. Wang T., Lin J., Ruf J. and Guidos M., "Transient Three-Dimensional Side Load Analysis of Out-of-Round Film Cooled Nozzles", *46th AIAA/ASME/SAE/ASEE Joint Propulsion Conference & Exhibit*, Nashville, Tennessee, (2010).

27. Wilcox D.C., "Turbulence Modeling for CFD", *3rd Edition, DCW Industries*, (2006).